

Equation of state and Goldstone-mode effects of the three-dimensional $O(2)$ model

J. Engels, S. Holtmann, T. Mendes and T. Schulze

Fakultät für Physik, Universität Bielefeld, D-33615 Bielefeld, Germany

Abstract

We investigate numerically the three-dimensional $O(2)$ model on 8^3 – 160^3 lattices as a function of the magnetic field H . In the low-temperature phase we verify the H -dependence of the magnetization M induced by Goldstone modes and determine M for $V \rightarrow \infty$ on the coexistence line both by extrapolation and by chiral perturbation theory. This enables us to calculate the corresponding critical amplitude. At T_c the critical scaling behaviour of the magnetization as a function of H is used to determine another critical amplitude. In both cases we find negative corrections-to-scaling. Our low-temperature results are well described by the perturbative form of the model's magnetic equation of state, with coefficients determined nonperturbatively from our data. The $O(2)$ scaling function for the magnetization is found to have a smaller slope than the one for the $O(4)$ model.

PACS : 64.60.C; 75.10.H; 12.38.Lg

Keywords: Goldstone modes; Equation of state; Scaling function; $O(N)$ models

E-mail: engels,holtmann,mendes,tschulze@physik.uni-bielefeld.de

1 Introduction

$O(N)$ models are of general relevance to condensed matter physics and to quantum field theory, because many physical systems exhibit a second-order phase transition with universal properties, which may be derived analytically from $O(N)$ symmetric effective field theories [1]. A further aspect of these theories is remarkable. Due to the existence of massless Goldstone modes in $O(N)$ models with $N > 1$ and dimension $2 < d \leq 4$ [2, 3] singularities are expected on the whole coexistence line $T < T_c, H = 0$, in addition to the known critical behaviour at T_c . For $N = 2$ and $d = 3$ there exists a rigorous proof [4]. Numerically these theoretical predictions have been recently confirmed by simulations of the $3d$ $O(4)$ model [5]. In the same article a parametrization of the equation of state including the Goldstone effect has been worked out and compared to perturbative predictions [6, 7]. Here we want to extend these numerical studies to the case of the $O(2)$ model. For the latter approximate representations of the equation of state have been derived, starting from high-temperature expansions [8].

Our interest in the $O(2)$ model is moreover motivated by its relation to the staggered formulation of quantum chromodynamics (QCD) on the lattice. At finite temperature QCD undergoes a chiral phase transition. For two degenerate light-quark flavors this transition is supposed to be of second order in the continuum limit and to belong to the same universality class as the $3d$ $O(4)$ model [9]-[11]. QCD lattice data have therefore been compared to the $O(4)$ scaling function, as determined numerically in [12]. For staggered fermions the comparison to $O(4)$ is still not conclusive [13]-[15], but results for Wilson fermions [16] seem to agree quite well with the predictions, though for the Wilson action the chiral symmetry is only restored in the continuum limit. In the staggered formulation a part of the chiral symmetry is remaining even for finite lattice spacing, and that is $O(2)$. For the test of lattice QCD with staggered fermions it is therefore also important to know the corresponding universal $O(2)$ scaling function or equation of state.

The $O(2)$ -invariant nonlinear σ -model (or XY model), which we want to investigate in the following is defined by

$$\beta \mathcal{H} = -J \sum_{\langle i,j \rangle} \mathbf{S}_i \cdot \mathbf{S}_j - \mathbf{H} \cdot \sum_i \mathbf{S}_i, \quad (1)$$

where i and j are nearest-neighbour sites on a d -dimensional hypercubic lattice, and \mathbf{S}_i is an 2 -component unit vector at site i . It is convenient to decompose the spin vector \mathbf{S}_i into a longitudinal (parallel to the magnetic field \mathbf{H}) and a transverse component

$$\mathbf{S}_i = S_i^{\parallel} \hat{\mathbf{H}} + \mathbf{S}_i^{\perp}. \quad (2)$$

The order parameter of the system, the magnetization M , is then the expectation

value of the lattice average S^{\parallel} of the longitudinal spin component

$$M = \langle \frac{1}{V} \sum_i S_i^{\parallel} \rangle = \langle S^{\parallel} \rangle . \quad (3)$$

On finite lattices and $H = 0$ system flips occur and lead to $\langle S^{\parallel} \rangle = 0$. Therefore one usually resorts to approximate order parameter definitions, as e.g. $\langle |S^{\parallel}| \rangle$ - see the discussion in Tapalov and Blöte [17]. Here this is unnecessary since we always work at finite H .

There are two types of susceptibilities. The longitudinal susceptibility is defined as usual by the derivative of the magnetization, whereas the transverse susceptibility corresponds to the fluctuation of the lattice average \mathbf{S}^{\perp} of the transverse spin component

$$\chi_L = \frac{\partial M}{\partial H} = V(\langle S^{\parallel 2} \rangle - M^2) , \quad (4)$$

$$\chi_T = V \langle \mathbf{S}^{\perp 2} \rangle . \quad (5)$$

Both susceptibilities are predicted to diverge on the coexistence line $T < T_c, H = 0$. The Goldstone singularities lead for all temperatures below T_c for small H to strong finite-size effects, which have been studied in the context of chiral perturbation theory for the three-dimensional $O(2)$ model already in [18]. An explicit check on the H -dependence of the magnetization for $V \rightarrow \infty$ close to $H = 0$ is however lacking. In comparison to the $O(4)$ model, we expect the Goldstone effects to be weaker, because we have only one transverse spin component in $O(2)$, not three like in $O(4)$. Another difference to $O(4)$ is that sizeable corrections to scaling appear in the XY model [19]. The determination of the universal equation of state of the three-dimensional $O(2)$ model, therefore requires a careful consideration of the corrections. We could have avoided the problems with these corrections by working, as it was done in Ref. [19] at $\lambda = 2.1$, instead of $\lambda = \infty$. For a better comparison to the $O(4)$ case [5], we chose however to use the same model definition. Also there is then no need for an additional modulus update.

The plan of the paper is as follows. In the next section we briefly discuss the perturbative predictions for the magnetization and the susceptibilities at low temperatures, the form and the analytic results for the magnetic equation of state. A more general review can be found in [5]. Our numerical results are presented in Section 3, the equation of state is determined and parametrized in Section 4. We close with a summary and our conclusions in Section 5.

2 Perturbative Predictions and Equation of State

For $T < T_c$ the system is in a broken phase, i.e. the magnetization $M(T, H)$ attains a finite value $M(T, 0)$ at $H = 0$. We explicitly assume here $H > 0$. As a consequence

the transverse susceptibility, which is directly related to the fluctuation of the Goldstone modes, diverges as H^{-1} when $H \rightarrow 0$ for all $T < T_c$. This is immediately clear from the identity [6]

$$\chi_T = \frac{M(T, H)}{H}, \quad (6)$$

which is valid for all values of T and H . It is non-trivial that also the longitudinal susceptibility is diverging on the coexistence line for $2 < d \leq 4$. The leading term in the perturbative expansion for $2 < d < 4$ is $H^{d/2-2}$ [2, 7]. The predicted divergence in $d = 3$ is thus

$$\chi_L(T < T_c, H) \sim H^{-1/2}. \quad (7)$$

This is equivalent to an $H^{1/2}$ -behaviour of the magnetization near the coexistence curve

$$M(T < T_c, H) = M(T, 0) + cH^{1/2}. \quad (8)$$

An interesting question is whether this form of the magnetization is compatible with the general Widom-Griffiths form of the equation of state [20] describing the critical behaviour in the vicinity of T_c . It is given by

$$y = f(x), \quad (9)$$

where

$$y \equiv h/M^\delta, \quad x \equiv t/M^{1/\beta}. \quad (10)$$

The variables t and h are the normalized reduced temperature $t = (T - T_c)/T_0$ and magnetic field $h = H/H_0$. We take the usual normalization conditions

$$f(0) = 1, \quad f(-1) = 0. \quad (11)$$

The critical exponents δ and β appearing in Eqs. 9 and 10 specify all the other critical exponents

$$d\nu = \beta(1 + \delta), \quad \gamma = \beta(\delta - 1), \quad \nu_c = \nu/\beta\delta. \quad (12)$$

Possible dependencies on irrelevant scaling fields and exponents are however not taken into account in Eq. 9, the function $f(x)$ is universal. Another way to express the dependence of the magnetization on t and h is

$$M = h^{1/\delta} f_G(t/h^{1/\beta\delta}), \quad (13)$$

where f_G is a scaling function. This type of scaling equation is used for comparison to QCD lattice data. The scaling forms in Eqs. (9) and (13) are clearly equivalent.

The equation of state (9) has been derived by Brézin et al. [6] to order ϵ^2 in the ϵ -expansion, where $\epsilon = 4 - d$. The resulting approximation has been considered by Wallace and Zia [7] in the limit $x \rightarrow -1$, i.e. at $T < T_c$ and close to the coexistence curve. In this limit the function is inverted to give $x + 1$ as a double expansion in powers of y and $y^{d/2-1}$

$$x + 1 = \tilde{c}_1 y + \tilde{c}_2 y^{d/2-1} + \tilde{d}_1 y^2 + \tilde{d}_2 y^{d/2} + \tilde{d}_3 y^{d-2} + \dots. \quad (14)$$

The coefficients \tilde{c}_1 , \tilde{c}_2 and \tilde{d}_3 are then obtained from the general expression of [6]. The above form is motivated by the H -dependence in the ϵ -expansion of χ_L at low temperatures [7]. In Section 4 we propose a fit of our Monte Carlo data to the perturbative form of the equation of state, using (14).

As for the large- x limit (corresponding to $T > T_c$ and small H), the expected behaviour is given by Griffiths's analyticity condition [20]

$$f(x) = \sum_{n=1}^{\infty} a_n x^{\gamma-2(n-1)\beta} . \quad (15)$$

3 Numerical Results

Our simulations are done on three-dimensional lattices with periodic boundary conditions and linear extensions $L = 8 - 160$ using the cluster algorithm of Ref. [21]. The value $J_c = 0.454165(4)$, obtained in simulations of the zero-field model [22], is used in the following. We have simulated at increasingly larger values of L at fixed values of $J = 1/T$ (i.e. at fixed temperature T) and H in order to eliminate finite-size effects.

As an example we show in Fig. 1 part of our data for the magnetization for low temperatures, at $J = 0.5$, 0.47 , and at J_c , plotted versus $H^{1/2}$. The picture is rather similar to the one obtained in $O(4)$ [5]: strong finite-size effects appear for small H and persist as one moves away from T_c , the results from the largest lattices are at first sight linear in $H^{1/2}$, as predicted by Eq. 8, below but not at T_c . A closer look at the curves reveals however subtle differences compared to the $O(4)$ case, which are confirmed by the attempt to determine the value of $M(T, H = 0)$ by a linear fit in $H^{1/2}$. Very close to $H = 0$ the fixed temperature curves become slightly flatter, leading to a higher value for $M(T, 0)$ than expected from the data at larger H values. This behaviour is more pronounced close to T_c than at lower temperatures. The determination of the magnetization in the thermodynamic limit ($V \rightarrow \infty$) on the coexistence line requires therefore more precise data and smaller values of H than for the $O(4)$ model. In order to extrapolate the data to $H \rightarrow 0$ and $V \rightarrow \infty$ we apply two different strategies. The first is to extend the linear form in $H^{1/2}$, Eq. 8, to a quadratic one [2]

$$M(T < T_c, H) = M(T, 0) + c_1 H^{1/2} + c_2 H , \quad (16)$$

and to fit the data from the largest lattices, which we assume to represent data on an infinite volume lattice, to this form. The second way to find $M(T, 0)$ is just opposite to the first. Here we exploit the L or volume dependence at fixed J and fixed small H to determine via chiral perturbation theory (CPT) the magnetization Σ of the continuum theory for $V \rightarrow \infty$, $H = 0$, which is related to $M(T, 0)$ by

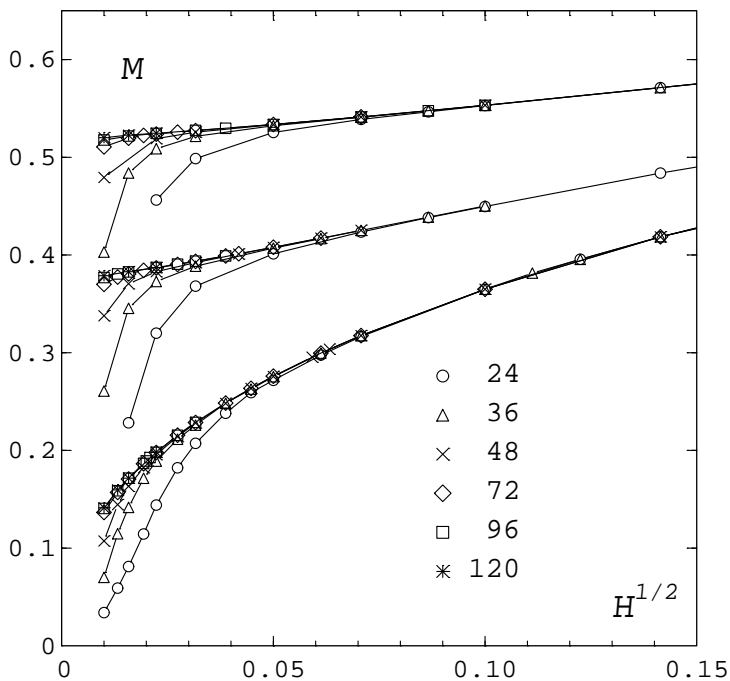


Figure 1: The magnetization as a function of $H^{1/2}$ in the low-temperature region for fixed $J = 0.5, 0.47$ and J_c , starting with the highest curve for various L .

$$M(T, 0) = \frac{\Sigma}{\sqrt{J}}. \quad (17)$$

According to the ϵ -expansion of CPT the quantity Σ and the Goldstone boson decay constant F are the only parameters which determine the finite-size corrections to the partition function to order $1/L^2$ [23]. We summarize the relevant formulae for the three-dimensional XY model from Ref. [18]. In our notation the magnetization is

$$M = \frac{\Sigma}{\sqrt{J}} u [\rho_1 \eta + 2\rho_2 \alpha^2], \quad (18)$$

where $u = \rho_1 \Sigma H V / \sqrt{J}$, $\alpha = 1/(F^2 L)$ and

$$\rho_1 = 1 + \frac{1}{2}\beta_1 \alpha + \frac{1}{8}(\beta_1^2 - 2\beta_2)\alpha^2; \quad \rho_2 = \frac{1}{4}\beta_2. \quad (19)$$

For a symmetric three-dimensional box $\beta_1 = 0.225785$ and $\beta_2 = 0.010608$. The parameter η is given in terms of modified Bessel functions as

$$\eta = \frac{I_1(u)}{u I_2(u)}. \quad (20)$$

By construction the ϵ -expansion is only applicable in a range where $m_\pi L \lesssim 1$ which translates into the condition

$$H \frac{\Sigma}{\sqrt{J}} \lesssim \left(\frac{F}{L}\right)^2. \quad (21)$$

In Fig. 2 we show the data for the magnetization as a function of $H^{1/2}$ for six fixed values of J in the low-temperature phase. We observe a remarkable coincidence of the fits according to Eq. 16 with the CPT results at $H = 0$. Details of the fits are presented in Table 1. The χ^2 per degree of freedom for the first fit type is in the range 0.01-0.5 . The corresponding numbers for the CPT fits are of the order of 1. Like for the $O(4)$ model we see in Fig. 2 that the region where M is linear in $H^{1/2}$ shrinks when T approaches T_c , the value of c_2 in Table 1 increases correspondingly. At $J = 0.460$ the fit parabola coincides only on a small piece with the largest volume data (here we simulated even on $L = 160$ lattices), the errors on c_1 and c_2 become large, though the value at $H = 0$ agrees again nicely with the CPT result. We have further convinced ourselves that $M(T, 0)$ can also be obtained from calculations at $H = 0$ with the modulus definition. The approach to the thermodynamic limit is here from above.

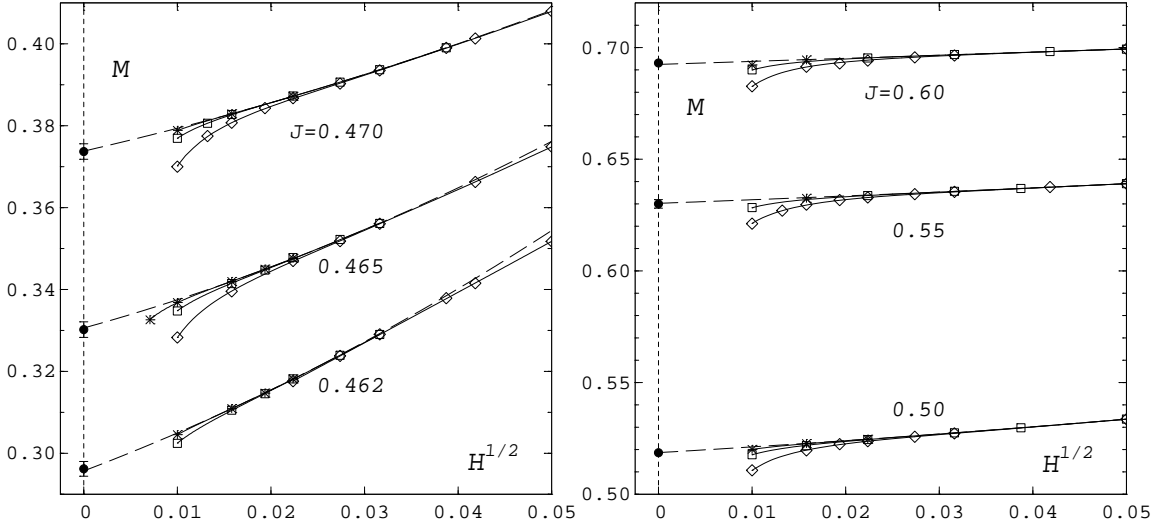


Figure 2: The magnetization vs. $H^{1/2}$ in the low-temperature region for fixed $J = 0.47, 0.465, 0.462$ (left plot) and $J = 0.6, 0.55, 0.5$ (right plot) and different L (notation as in Fig.1). The filled circles are the results from CPT, the dashed lines the fits according to Eq. 16. The solid lines connecting the data are from reweighting.

In the neighbourhood of the critical temperature the results for $M(T, 0)$ should show the usual critical behaviour. Contrary to the $O(4)$ case we expect here a sizeable correction to the leading scaling behaviour [19]. In order to determine the critical amplitude B we therefore make the following ansatz

$$M(T \lesssim T_c, H = 0) = B(T_c - T)^\beta [1 + b_1(T_c - T)^{\omega\nu} + b_2(T_c - T)]. \quad (22)$$

As an input we take the critical exponents from Ref. [19]

$$\beta = 0.3490(6), \quad \nu = 0.6723(11), \quad \omega = 0.79(2). \quad (23)$$

$J = 1/T$	$M(T, 0)$	c_1	c_2	$10^4 \cdot H$	Σ/\sqrt{J}	L
0.460	0.2724(27)	0.53(30)	21.9(80)	2-5	0.2720(27)	12-40
0.462	0.2957(03)	0.865(30)	6.18(82)	2-5	0.2962(18)	12-36
0.465	0.3306(02)	0.633(17)	5.58(36)	3-10	0.3302(19)	12-40
0.470	0.3738(01)	0.526(03)	3.24(05)	3-15	0.3737(19)	8-40
0.500	0.5186(01)	0.244(02)	1.11(02)	8-75	0.5186(12)	16-48
0.550	0.6303(01)	0.157(01)	0.38(01)	10-50	0.6300(19)	12-56
0.600	0.6925(01)	0.133(01)	0.09(01)	16-75	0.6931(07)	8-64

Table 1: Parameters of the fit of $M(T, H)$ to Eq. 16 in the H -range of column 5 and the results of the CPT fit for $H = 0.0001$ in the L -range of column 7.

A fit of all points of Table 1, apart from the one at $J = 0.46$, using the form (22) leads to the result $B = 0.945(5)$, $b_1 = -0.053(23)$ and $b_2 = -0.098(23)$. In Fig. 3a we show this fit and also the leading term separately.

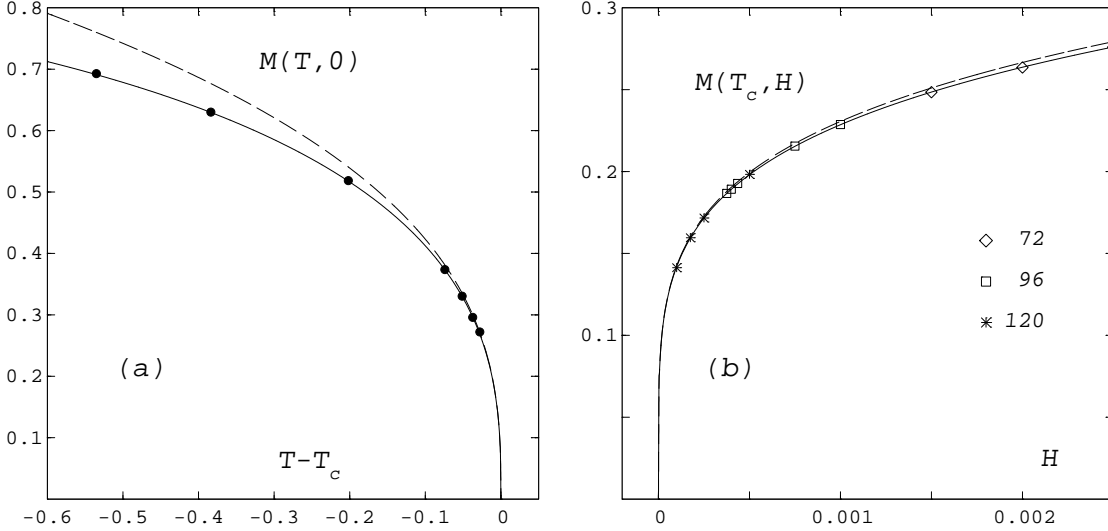


Figure 3: (a) The magnetization on the coexistence line versus $T - T_c$, the points are from Table 1, the solid line is the fit (22), the dashed line its leading part. (b) The magnetization at T_c as a function of H , the line is the fit (24), the dashed line the leading part.

As the critical point is reached the H -dependence of the magnetization changes to satisfy critical scaling. We therefore fit the data from the largest lattice sizes at T_c to the form

$$M(T_c, H) = d_c H^{1/\delta} [1 + d_c^1 H^{\omega\nu_c}] . \quad (24)$$

A further term proportional to H is unnecessary, because the corrections to scaling are much smaller here, than on the coexistence line. The largest L data can be fitted very well with the ansatz (24) and the critical exponents as input, as can be seen in Fig. 3b. We find $d_c = 0.978(2)$ and $d_c^1 = -0.075(5)$.

We have performed in addition some simulations in the high temperature phase of the model. Here the finite size effects are rather small. In Fig. 4 we show the results. One observes that with increasing T (decreasing J) the region of linear dependence on H of the magnetization becomes larger.

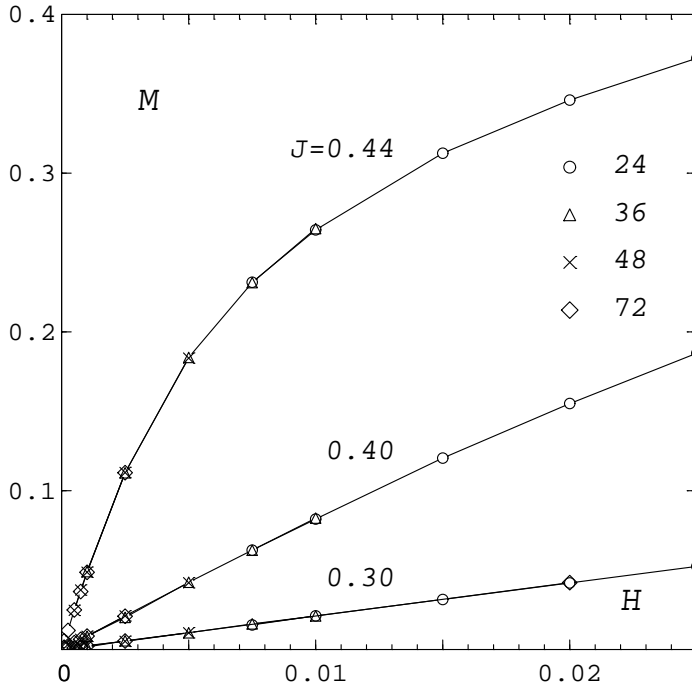


Figure 4: The magnetization as a function of H in the high-temperature region for fixed $J = 0.44, 0.4$ and 0.3 , starting with the highest curve for various L .

4 Determination of the Equation of State

In the last section we derived from our Monte Carlo data the magnetization in the thermodynamic limit. At temperatures below T_c this was achieved for the larger H values by simply performing simulations on lattices with increasing size until all volume dependence was gone. For the small H region down to $H = 0$ we took then advantage of the Goldstone effect to extrapolate our data and confirmed this by the CPT results for Σ . In the high-temperature phase we reached the thermodynamic limit already on lattices with $L \leq 72$ for all H values.

The two critical amplitudes B and d_c can now be utilized to normalize temperature

and magnetic field according to Eq. (11). We find from our fits (22) and (24)

$$T_0 = B^{-1/\beta} = 1.18(2) , \text{ and } H_0 = d_c^{-\delta} = 1.11(1) . \quad (25)$$

As mentioned already, the equation of state does not account for possible corrections to scaling. A more general form of Eq. (13) is

$$Mh^{-1/\delta} = \Psi(th^{-1/\beta\delta}, h^{\omega\nu_c}) . \quad (26)$$

Expanding the function Ψ in $h^{\omega\nu_c}$ leads to

$$Mh^{-1/\delta} = f_G(th^{-1/\beta\delta}) + h^{\omega\nu_c} f_G^{(1)}(th^{-1/\beta\delta}) + \dots . \quad (27)$$

In order to obtain the scaling function f_G we therefore perform quadratic fits to our data in $h^{\omega\nu_c}$ at fixed values of $th^{-1/\beta\delta}$ in the low-temperature region, where the corrections are strong. Fortunately, the corrections are very small in the high-temperature region and the data scale directly. Altogether data with $H \leq 0.0075$ and $0.43 \leq J \leq 0.55$ were used for this purpose. In Fig. 5 we have plotted the uncorrected and the final results for the scaling function f_G .

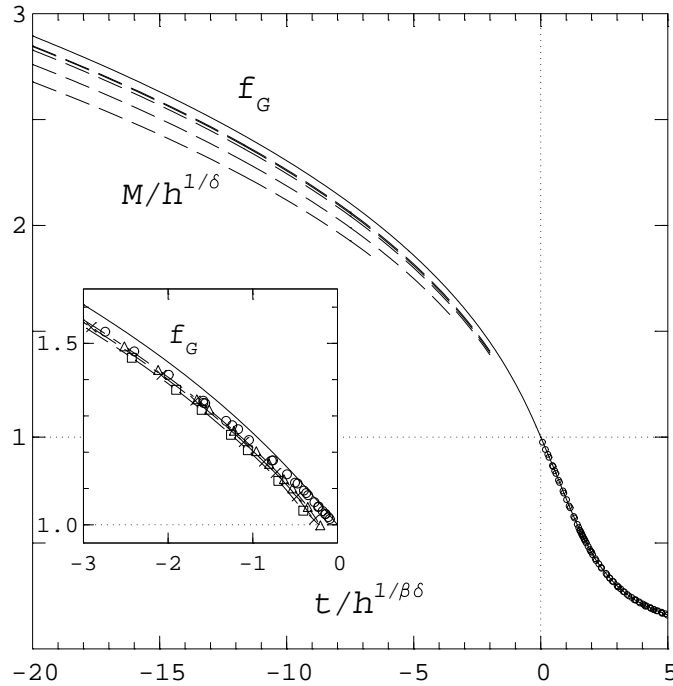


Figure 5: The scaling function f_G , Eq. (13), (solid line). Also shown are the results for $M/h^{1/\delta}$ at fixed values of $J = 0.55, 0.50, 0.47, 0.465$ and 0.462 (dashed lines) which were used for the extrapolation, starting with the lowest curve. The circles are single data points. The inset shows the low-temperature region close to T_c , with data for $J \leq 0.46$ (circles), 0.462 (triangles), 0.465 (crosses) and 0.47 (squares).

Like in the case of $O(4)$ [5] we want to describe the low-temperature part of the equation of state by its perturbative form as discussed in Section 2, but with non-perturbative coefficients. We then want, again as in Ref. [5], to interpolate this

result with a fit to the large- x form (15). The variables x and y are simply related to the scaling function f_G and its argument by

$$y = f_G^{-\delta}, \quad x = (t/h^{1/\beta\delta}) f_G^{-1/\beta}. \quad (28)$$

We first perform a fit to x in the interval $[-1, 1.4]$ (which corresponds to $y \in [0, 3]$) with the three leading terms in (14)

$$x_1(y) + 1 = (\tilde{c}_1 + \tilde{d}_3) y + \tilde{c}_2 y^{1/2} + \tilde{d}_2 y^{3/2}. \quad (29)$$

In the fit we require $\tilde{d}_2 = 1 - (\tilde{c}_1 + \tilde{d}_3 + \tilde{c}_2)$ to fix the normalization $y(0) = 1$. We obtain

$$\tilde{c}_1 + \tilde{d}_3 = 0.352(30), \quad \tilde{c}_2 = 0.592(10). \quad (30)$$

The fit describes the corrected scaling function at $T < T_c$ and the direct data in the high temperature phase up to $x \approx 1.7$. This confirms, as in $O(4)$, that the expression (14) is valid also away from $x \approx -1$. Our coefficients can be compared to those calculated perturbatively for $N = 2$ in Ref. [7]

$$\tilde{c}_1 + \tilde{d}_3 = 0.818, \quad \tilde{c}_2 = 0.229. \quad (31)$$

The result (30) is much closer to the coefficients found in $O(4)$ [5] than to the ϵ -expansion results (31), though the Goldstone effect is decreasing somewhat with decreasing N : \tilde{c}_2 and the x region where the ansatz (29) is valid are a little smaller.

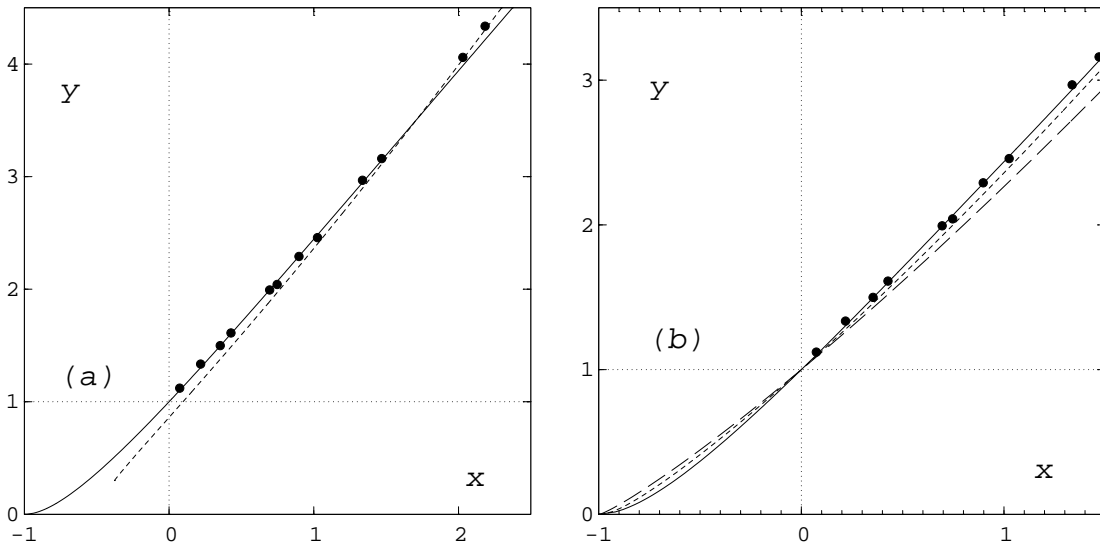


Figure 6: (a) The function $y = f(x)$ from fits at small x (solid line) and at large x (dashed line). (b) The interpolation (34) for $f(x)$ (solid line), and the parametrizations (A) (short dashes) and (B) (long dashes), $n = 1$ of $f(x)$ from Ref. [8]. In both parts we show high-temperature data (filled circles).

For large x we have done a 2-parameter fit of the behaviour (15), in the corresponding form for x in terms of y

$$x_2(y) = a y^{1/\gamma} + b y^{(1-2\beta)/\gamma} . \quad (32)$$

Considering data points with y in the interval [4,23000] we find

$$a = 1.2595(30) , \quad b = -1.163(20) . \quad (33)$$

Expression (32) describes the data for $x > 1.5$. The small- and large- x curves cover the whole range of values of x remarkably well. The two curves overlap around $y \approx 3.5$. This is shown in Fig. 6a. We therefore interpolate them smoothly with the ansatz

$$x(y) = x_1(y) \frac{y_0^6}{y_0^6 + y^6} + x_2(y) \frac{y^6}{y_0^6 + y^6} , \quad (34)$$

where $y_0 = 3.5$. In Fig. 6b we compare our interpolation (34) of the equation of state to the high-temperature data and to two parametric forms for $f(x)$ obtained from the high-temperature expansion in Ref. [8]. According to the authors [24], the difference between these two curves gives an idea of the uncertainty of their approach. For large x this difference can be traced back to the uncertainty in the universal amplitude ratio R_χ (Eq. (49) of Ref. [8]), which was determined in [8] to $R_\chi = 1.4(1)$, that is with a 7% error. In fact, R_χ is related to the quantity a of our large- x parametrization by

$$R_\chi = a^\gamma = 1.356(4) , \quad (35)$$

which is in agreement with the result from Ref. [8]. Their low temperature parameter c_f may be calculated from our value of \tilde{c}_2 and amounts to $c_f = 2.85(7)$. Finally we show in Fig. 7 the scaling function f_G obtained parametrically from $x(y)$ in (34) and the corresponding scaling function for $O(4)$. As can be seen from Fig. 7, the dependence on $t/h^{1/\delta\beta}$ is similar, but the $O(2)$ curve is flatter than the one for $O(4)$.

5 Summary and Conclusions

We have simulated the three-dimensional $O(2)$ model on cubic lattices as a function of the magnetic field H and the temperature T . From the behaviour of the measured magnetization M below the critical temperature T_c and close to the coexistence line ($H = 0$), we could clearly verify the Goldstone-mode effects. This was done in two independent ways which led to the same values $M(T < T_c, H \rightarrow 0)$ for the magnetization in the thermodynamic limit $V \rightarrow \infty$: on one hand we were able to profit by the observed Goldstone behaviour to extrapolate our data to $H \rightarrow 0$ and on the other hand this result was confirmed from the finite-size dependence induced by the Goldstone modes, using chiral perturbation theory.

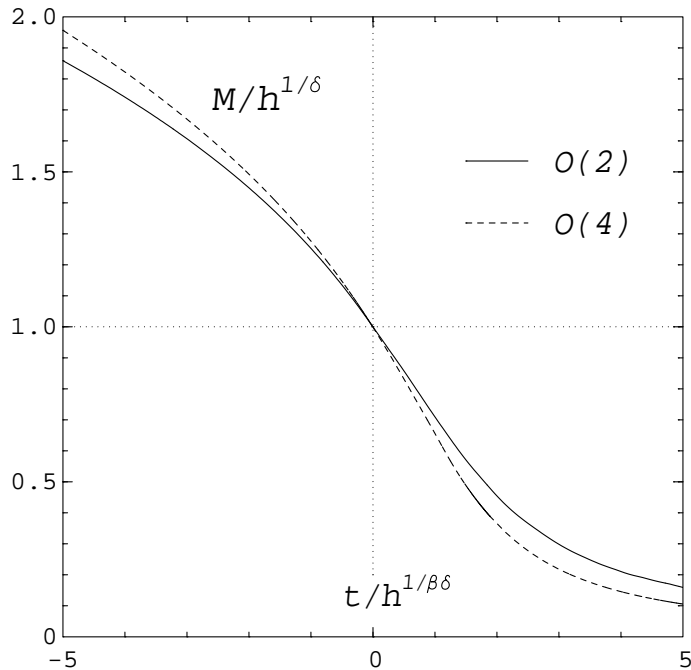


Figure 7: The scaling function $f_G = M/h^{1/\delta}$ for the $O(2)$ model (solid line) and the $O(4)$ model (dashed line).

The M values on the coexistence line were subsequently used to calculate the critical amplitude B of the magnetization. Not unexpectedly, we found here strong corrections to scaling. On the critical line $T = T_c$ we computed then the second critical amplitude d_c of the magnetization. Here, the corrections to scaling are less pronounced ; in the high-temperature phase they are unimportant.

The problem with corrections to scaling appeared again in the determination of the equation of state in the low-temperature phase. By generalizing the scaling equation to include possible corrections, we were able to derive the universal form of the equation of state for the $O(2)$ model from our data. This form was then analyzed in a similar manner as it was done for the $O(4)$ model in Ref. [5]. In particular, we found again an efficient parametrization of the equation of state in the low x region with the perturbative form (29), which is based on expansion (14) by Wallace and Zia [7]. The effect due to the Goldstone modes is nearly as large as in the $O(4)$ case, as can be seen from the coefficient \tilde{c}_2 and much larger than the prediction from the ϵ -expansion.

Like for $O(4)$ we found a very good large- x fit to the high-temperature data. The coefficient a obtained from the fit implies a value of $R_\chi = 1.356(4)$, in agreement with parametrizations of the equation of state by Campostrini et al. [8]. A further, indirect check of the equation of state is the computation of the universal ratio A_+/A_- . This requires however an integration of the magnetization with respect to h and derivatives with respect to t . We shall consider this in the near future.

Upon interpolation with the low- x curve, a complete description for the equation of state is obtained, which can be plotted parametrically also for the scaling function. In Ref. [15] the lattice QCD data of the MILC Collaboration for $N_\tau = 4$ were compared to the $O(4)$ scaling function. The test failed because the data were indicating a steeper scaling function. Since the $O(2)$ scaling function is flatter than the one for $O(4)$, the situation will be worse there. A way out may be the comparison to finite-size-scaling functions, since lattice QCD is presumably far from the thermodynamic limit. We are investigating this currently.

Acknowledgements

We thank Attilio Cucchieri for helpful suggestions and comments. This work was supported by the Deutsche Forschungsgemeinschaft under Grant No. Ka 1198/4-1.

References

- [1] J. Zinn-Justin, *Precise determination of critical exponents and equation of state by field theory methods*, hep-th/0002136.
- [2] J. Zinn-Justin, *Quantum Field Theory and Critical Phenomena*, Clarendon Press, Oxford, 1996.
- [3] R. Anishetty, R. Basu, N.D. Hari Dass and H.S. Sharatchandra, *Int. J. Mod. Phys. A***14** (1999) 3467.
- [4] J.L. Lebowitz and O. Penrose, *Phys. Rev. Lett.* **35** (1975) 549;
F. Dunlop and C.M. Newman, *Commun. Math. Phys.* **44** (1975) 223.
- [5] J. Engels and T. Mendes, *Nucl. Phys.* **B572** (2000) 289.
- [6] E. Brézin, D.J. Wallace and K.G. Wilson, *Phys. Rev.* **B7** (1973) 232.
- [7] D.J. Wallace and R.K.P. Zia, *Phys. Rev.* **B12** (1975) 5340.
- [8] M. Campostrini, A. Pelissetto, P. Rossi and E. Vicari, cond-mat/0001440.
- [9] R. Pisarsky and F. Wilczek, *Phys. Rev.* **D29** (1984) 338.
- [10] F. Wilczek, *J. Mod. Phys.* **A7** (1992) 3911.
- [11] K. Rajagopal and F. Wilczek, *Nucl. Phys.* **B399** (1993) 395.
- [12] D. Toussaint, *Phys. Rev.* **D55** (1997) 362.
- [13] E. Laermann, *Nucl. Phys. B (Proc. Suppl.)* **63A-C** (1998) 114.
- [14] S. Aoki et al. (JLQCD Collaboration), *Phys. Rev.* **D57** (1998) 3910.

- [15] C. Bernard et al. (MILC Collaboration), Phys. Rev. D**61** (2000) 054503.
- [16] A. Ali Khan et al. (CP-PACS Collaboration), Nucl. Phys. B (Proc.Suppl.)**83-84** (2000) 360.
- [17] A.L. Talapov and H.W.J. Blöte, J. Phys. A**29** (1996) 5727.
- [18] S. Tominaga and H. Yoneyama, Phys. Rev. B**51** (1995) 8243.
- [19] M. Hasenbusch and T. Török, J. Phys. A**32** (1999) 6361.
- [20] R.B. Griffiths, Phys. Rev. **158** (1967) 176.
- [21] I. Dimitrović, P. Hasenfratz, J. Nager and F. Niedermayer, Nucl. Phys. B**350** (1991) 893.
- [22] H.G. Ballesteros, L.A. Fernández, V. Martín-Mayor and A. Muñoz Sudupe, Phys. Lett. B**387** (1996) 125.
- [23] P. Hasenfratz and H. Leutwyler, Nucl. Phys. B**343** (1990) 241.
- [24] M. Campostrini, A. Pelissetto, P. Rossi and E. Vicari, private communication.